Physica D 425 (2021) 132930

Contents lists available at ScienceDirect

Physica D

journal homepage: www.elsevier.com/locate/physd

Persisting asymmetry in the probability distribution function for a random advection–diffusion equation in impermeable channels

Roberto Camassa [a], Lingyun Ding [a], Zeliha Kilic [b], Richard M. McLaughlin [a,*]

[a] Department of Mathematics, University of North Carolina, Chapel Hill, NC, 27599, United States
[b] Center for Biological Physics, Arizona State University, Tempe, AZ, 85282, United States

ARTICLE INFO

Article history:
Received 10 September 2020
Received in revised form 3 March 2021
Accepted 12 April 2021
Available online 14 May 2021
Communicated by M. Jolly

Keywords:
Random shear flow
Skewness
Turbulent transport
Passive scalar

ABSTRACT

In this paper, we study the effect of impermeable boundaries on the symmetry properties of a random passive scalar field advected by random flows. We focus on a broad class of nonlinear shear flows multiplied by a stationary, Ornstein–Uhlenbeck (OU) time varying process, including some of their limiting cases, such as Gaussian white noise or plug flows. For the former case with linear shear, recent studies (Camassa et al., 2019) numerically demonstrated that the decaying passive scalar's long time limiting probability distribution function (PDF) could be negatively skewed in the presence of impermeable channel boundaries, in contrast to rigorous results in free space which established the limiting PDF is positively skewed (McLaughlin and Majda, 1996). Here, the role of boundaries in setting the long time limiting skewness of the PDF is established rigorously for the above class using the long time asymptotic expansion of the N-point correlator of the random field obtained from the ground state eigenvalue perturbation approach proposed in Bronski and McLaughlin (1997). Our analytical result verifies the conclusion for the linear shear flow obtained from numerical simulations in Camassa et al. (2019). Moreover, we demonstrate that the limiting distribution is negatively skewed for any shear flow at sufficiently low Péclet number. We demonstrate the convergence of the Ornstein–Uhlenbeck case to the white noise case in the limit $\gamma \to \infty$ of the OU damping parameter, which generalizes the results for free space in Resnick (1996) to the channel domain problem. We show that the long time limit of the first three moments depends explicitly on the value of γ, which is in contrast to the conclusion in Vanden Eijnden (2001) for the limiting PDF in free space. To find a benchmark for theoretical analysis, we derive the exact formula of the N-point correlator for a flow with no spatial dependence and Gaussian temporal fluctuation, generalizing the results of Bronski et al. (2007). The long time analysis of this formula is consistent with our theory for a general shear flow. All results are verified by Monte-Carlo simulations.

1. Introduction

Partial differential equations (PDEs) with random coefficients have been the focus of many studies as they occur in a variety of mathematical models of physical systems. Some examples from this class of PDEs include passive scalar (e.g., fluid temperature or solute concentration) advection by random fluid flows [1–4], linear and nonlinear Schrödinger equations with random potentials [5,6], light propagating through random media [7] and random water waves impinging on a step [8,9].

Motivated by the Chicago convection experiments [10], random passive scalars have been intensely studied as a simplified model for intermittency in fluid turbulence that, while enjoying a linear evolution, retain many statistical closure features reminiscent of problems in fluid turbulence [4,11–15]. In particular, the case of diffusing passive scalar advected by a rapidly fluctuating Gaussian random fluid flow has been the focus of much analysis as the moment closure problem is bypassed in the white noise limit [1,2,4,16,16–20]. Notably, the availability of closed evolution equations for the statistical correlators led to the discovery that a diffusing passive scalar could inherit a heavy-tailed, non-Gaussian PDF from a Gaussian random fluid flow [1,17,19,21]. Additional studies have explored the role played by finite or infinite correlation times in a random shear flow [22,23]. This generic non-Gaussian behavior in a passive scalar has been termed 'scalar intermittency'. Subsequently, similar findings have been observed in field experimental data, such as atmospheric wind measurements [24] as well as observations of stratospheric inert tracers [25].

* Corresponding author.
E-mail addresses: camassa@amath.unc.edu (R. Camassa), dingly@live.unc.edu (L. Ding), zkilic@asu.edu (Z. Kilic), rmm@email.unc.edu (R.M. McLaughlin).

https://doi.org/10.1016/j.physd.2021.132930
0167-2789/

Further investigations have provided more in depth understanding of how the non-Gaussian measure is dynamically attained [26], and further explored the case of a passive scalar advected by a shear-free temporally fluctuating wind, where the entire probability measure can be determined at any time [27]. This further exhibited how the diffusivity adjusts the location of singularities in the probability measure. Additional studies contrasted the scalar PDF inherited by an unbounded linear shear with that of a bounded, periodic shear flow [18]. This established that for integrable random initial data the PDF would 'Gaussianize' at long times, whereas random wave initial data whose Fourier transform is zero in a neighborhood of the origin would produce divergent flatness factors in the same long time limit.

While theoretically interesting, unbounded domains are of course unattainable in actual experiments, and the effects of boundaries need to be included for realistic models. Recently, the role of impermeable boundaries has been explored in a channel geometry with deterministic initial conditions [28]. This work established the surprising role that the boundary conditions play in setting the skewness of the PDF. McLaughlin and Majda [1] established that in free-space, with deterministic initial data, the long time PDF skewness would be strictly positive, whereas Monte-Carlo simulations in [28] have demonstrated that with no-flux boundary conditions in a channel geometry, the long time PDF skewness can be negative. Further, it has been shown in [28] that such flows could be physically realized by a randomly moving wall. More recently, the enhanced diffusion [29] and third spatial Aris moment [30] induced by a periodically moving wall was studied experimentally and theoretically [31], where it is noteworthy that the flows' temporal dependence is non-multiplicative.

Inspired from the ground state energy expansion strategy to handle more realistic flows (e.g. periodic flows in [18]) and the recent numerical findings provided in [28], here we rigorously establish that impermeable boundary conditions in a channel geometry can yield a scalar PDF with negative long-time skewness. We do so for a range of molecular diffusivities and for arbitrary nonlinear shear layers multiplied by a stationary Ornstein–Uhlenbeck process, through an explicit calculation of the long time scalar skewness asymptotics. Further, we gain insight into the role of the correlation time in the underlying stochastic process in the dynamic evolution of the scalar skewness, and in particular establish that longer correlation times yield increased transient dynamics.

The paper is organized as follows: In Section 2, we formulate the problem of the evolution of the passive scalar field advected by a nonlinear shear layer multiplied by an Ornstein–Uhlenbeck random process with an impermeable boundary and introduce some important conclusions of this scalar intermittency model. In Section 3, we derive a long time asymptotic expansion of the N-point correlation function of the scalar field by the perturbation theory and the differential operator spectral theory. Based on the N-point correlation function, we study the PDF of the scalar and show how the flow controls the asymmetry of PDF, which rigorizes and generalizes the conclusions in the article [28]. We perform numerical simulations for the linear shear flow multiplied by an OU process with different parameters by using the backward Monte-Carlo method described in Appendix A.1. The numerical results quantitatively demonstrate the validity of the formulae we derive in this section. In Section 4, we study the model with a spatially uniform, temporally Gaussian fluctuated shear flow. Being a special case of shear flow, the spatially uniform structure allows access to the exact formulae of the Green's function and the N-point correlation function. These are consistent with the long time asymptotic expansion in Section 2 and are verified by Direct Monte-Carlo (DMC) simulation proposed in [28]. In Section 5, we summarize the conclusions from the findings in the paper and briefly discuss future studies.

2. Setup and background of the problem for scalar intermittency

We will study intermittency in the following random advection–diffusion equation with deterministic initial condition $T_0(x, y)$ and impermeable channel boundary conditions,

$$\frac{\partial T}{\partial t} + \xi(t)u(y)\frac{\partial T}{\partial x} = \kappa \Delta T, \quad T(x, y, 0) = T_0(x, y), \quad \left.\frac{\partial T}{\partial y}\right|_{y=0,L} = 0, \tag{1}$$

where the domain is $\{(x, y)|x \in \mathbb{R}, y \in [0, L]\}$, L is the gap thickness of the channel, κ is the diffusivity, $\xi(t)$ is a zero-mean, Gaussian random process with the correlation function given by $\langle \xi(t)\xi(s)\rangle = R(t, s)$. The time dependent random shear flow can originate from either a time varying pressure field, or by randomly moving portions of the boundary. Such a shear flow can be obtained by solving the Navier–Stokes equations with boundary conditions matching the wall velocity $\xi(t)$, see section 2 of [28] for more details. Our recent study [31] regarding tracer dispersion induced by a periodically moving wall led to the development of a realizable experimental framework, where the computer-controlled robotic arm we developed can move the wall randomly and generate the desired random shear flow with suitable parameters of the fluid and the channel. In this experimental configuration, $T(x, y, t)$ is the concentration of the tracer which can be measured by optical methods. Hence, it is natural to consider the initial condition with the constraints $T_0(x, y) \geq 0$ and $\int_{-\infty}^{\infty} dx \int_0^L dy T_0(x, y) < \infty$.

We note that in this study we only consider shear flows whose spatial averages are non-zero, such as would arise in an experiment in which only one channel wall is moved, with statistics measured in the laboratory frame. We note that the symmetric case involving two oppositely moving walls requires higher order asymptotics to compute leading order long time skewness limits and will be explored in future work.

In this paper, two additional simplifying assumptions about flows are made. 1) $\xi(t)$ is a Gaussian white noise in time so that $R(t, s) = g^2\delta(t - s)$, or 2) $\xi(t)$ is a stationary Ornstein–Uhlenbeck process with the damping parameter γ and dispersion parameter σ, which is the solution of stochastic differential equation (SDE) $d\xi(t) = -\gamma\xi(t)dt + \sigma dB(t)$ with the initial condition $\xi(0) \sim \mathcal{N}(0, \sigma^2/2\gamma)$. Here $B(t)$ is the standard Brownian motion and $\mathcal{N}(a, b)$ is the normal distribution with mean a and variance b. The correlation function of $\xi(t)$ is $R(t, s) = \frac{\sigma^2}{2\gamma}e^{-\gamma|t-s|}$. γ^{-1} is often referred to as the correlation time of the OU process. It is easy to check that the stationary OU process converges to the Gaussian white noise process as the correlation time vanishes with fixed σ/γ. The underlying Brownian motion, $B(t)$, in the SDE introduces a canonical probability space (Ω_B, P_B) equipped with the filtration $\mathscr{F}_B$ that is induced by the Brownian motion itself [32].

Notice that $\gamma \sim \text{Time}^{-1}$, $\sigma \sim \text{Time}^{-\frac{3}{2}}$. With the change of variables,

$$\begin{aligned}
&Lx' = x, \quad Ly' = y, \quad \frac{L^2}{\kappa}t' = t, \quad g = \sigma/\gamma,\\
&\frac{g\sqrt{\kappa}}{L}\xi'(t') = \xi(t), \quad \frac{\kappa}{L^2}\gamma' = \gamma, \quad U = Lg^2, \quad Uu'(y')\xi'(t') = u(y)\xi(t),\\
&T'(x', y', t')L^{-2}\int_{-\infty}^{\infty} dx \int_0^L dy T_0(x, y) = T(x, y, t),\\
&T_0'(x', y')L^{-2}\int_{-\infty}^{\infty} dx \int_0^L dy T_0(x, y) = T_0(x, y),
\end{aligned} \tag{2}$$

we can drop the primes without confusion and obtain the nondimensionalized version of (1):

$$\frac{\partial T}{\partial t}+\mathrm{Pe}\,\xi(t)u(y)\frac{\partial T}{\partial x}=\Delta T,\quad T(x,y,0)=T_0(x,y),\quad \left.\frac{\partial T}{\partial y}\right|_{y=0,1}=0, \tag{3}$$

where the domain is $\{(x,y)|x\in\mathbb{R},y\in[0,1]\}$, and we have introduced the Péclet number $\mathrm{Pe}=UL/\kappa=L^2g^2/\kappa$. When $\xi(t)$ is the white noise process, the correlation function of $\xi(t)$ is $R(t,s)=\delta(t-s)$. Conversely, when $\xi(t)$ is the stationary Ornstein–Uhlenbeck process, the underlying SDE becomes $\mathrm{d}\xi(t)=-\gamma\xi(t)\mathrm{d}t+\mathrm{d}B(t)$ with the initial condition $\xi(0)\sim\mathcal{N}(0,\frac{\gamma}{2})$, and the correlation function of $\xi(t)$ is $R(t,s)=\frac{\gamma}{2}e^{-\gamma|t-s|}$.

Define the N-point correlation function Ψ_N of the scalar field $T(x,y,t)$: $\mathbb{R}^{2N}\times\mathbb{R}^+\to\mathbb{R}$ by $\Psi_N(\mathbf{x},\mathbf{y},t)=\left\langle\prod_{j=1}^N T(x_j,y_j,t)\right\rangle_{\xi(t)}$, where the bold letters denote the N-tuple of the coordinates, $\mathbf{x}=(x_1,x_2,\ldots,x_N)$, $\mathbf{y}=(y_1,y_2,\ldots,y_N)$. Here, the bracket $\langle\cdot\rangle_{\xi(t)}$ denotes the ensemble averaging with respect to the stochastic process $\xi(t)$ on the probability space $(\Omega_B,\mathscr{F}_B,P_B)$ that we introduced before. The Ψ_N associated with the free space version of (1) is known for some special flows. When $\xi(t)$ is the Gaussian white noise process, Majda [16] showed that Ψ_N satisfies the following evolution equation,

$$\frac{\partial\Psi_N}{\partial t}=\Delta_{2N}\Psi_N+\frac{\mathrm{Pe}^2}{2}\left(\sum_{j=1}^N u\left(y_j\right)\frac{\partial}{\partial x_j}\right)^2\Psi_N,\ \Psi_N(\mathbf{x},\mathbf{y},0)=\prod_{j=1}^N T_0(x_j,y_j), \tag{4}$$

where Δ_{2N} is the Laplacian operator in $2N$ dimensions $\Delta_{2N}=\sum_{j=1}^N\frac{\partial^2}{\partial x_j^2}+\frac{\partial^2}{\partial y_j^2}$. When $u(y)=y$, Majda [16] derived the exact expression of Ψ_N. A rotation of coordinates reduces the N-dimensional problem to a one-dimensional problem. Then the solution of (4) is available via Mehler's formula. Based on this exact N-point correlation function, the distribution of the scalar field advected by a linear shear flow has been studied for deterministic and random initial data. The non-Gaussian behaviors of PDF have been reported in [1,19,21].

When $\xi(t)$ is the stationary Ornstein–Uhlenbeck process, by introducing an extra variable z to represent the initial value of the stationary OU process, Resnick [22] showed that $\Psi_N(\mathbf{x},\mathbf{y},t)=\frac{1}{\sqrt{\pi}}\int_{-\infty}^{+\infty}\mathrm{d}z\psi_N(\mathbf{x},\mathbf{y},z,t)e^{-z^2}$, where $\psi_N(\mathbf{x},\mathbf{y},z,t)$ satisfies the following partial differential equation

$$\frac{\partial\psi_N}{\partial t}+\mathrm{Pe}\sqrt{\gamma}z\sum_{j=1}^N u(y_j)\frac{\partial\psi_N}{\partial x_j}+\gamma z\frac{\partial\psi_N}{\partial z}=\Delta_{2N}\psi_N+\frac{\gamma}{2}\frac{\partial^2\psi_N}{\partial z^2},$$
$$\psi_N(\mathbf{x},\mathbf{y},z,0)=\prod_{j=1}^N T_0(x_j,y_j). \tag{5}$$

When $u(y)=y$, Resnick derived the exact expression for Ψ_N via the same strategy Majda used for solving (4) and showed it converges to the solution of (4) in the limit $\gamma\to\infty$ of the OU damping parameter.

These results are all derived in free-space. The N-point correlation function Ψ_N for the boundary value problem (3) is unknown even for simple-geometry domains. For periodic boundary conditions, Bronski and McLaughlin [18] carried out a second order perturbation expansion for the ground state of periodic Schrödinger equations to analyze the inherited probability measure for a passive scalar field advected by periodic shear flows with a multiplicative white noise. In [28], (3) was studied with the flow $u(y)=y\xi(t)$ where $\xi(t)$ is the white noise process. A dramatically different long time state resulting from the existence of the impermeable boundaries was found. In particular, the PDF of the scalar in the channel case has negative skewness, in stark contrast to free space, where the limiting skewness is positive. Inspired by the observation reported in [28], we further explore here the PDF of the advected scalar in the presence of impermeable boundaries by the perturbation method introduced in [18]. Briefly, the long time behavior of the Fourier transform of N-point correlation function $\hat{\Psi}_N$ of the scalar field is dominated by the neighborhood of the zero wavenumber $\mathbf{k}=\mathbf{0}$. This observation reduces the series expansion of $\hat{\Psi}_N$ to a single multi-dimensional Laplace type integral. Then, the standard asymptotic analysis and inverse Fourier transform yield the long time asymptotic expansion of Ψ_N.

3. Long-time asymptotics: ground state energy expansion in channel geometry

For bounded domains, the N-point correlation function Ψ_N inherits the impermeable boundary condition from the scalar field. Since the velocity field in (4) and (5) is a shear layer, the Fourier transform $\hat{f}(\mathbf{k})=(2\pi)^{-\frac{N}{2}}\int_{\mathbb{R}^N}\mathrm{d}\mathbf{x}e^{-\mathrm{i}(\mathbf{x}\cdot\mathbf{k})}f(\mathbf{x})$ yields a parabolic Schrödinger equation

$$\frac{\partial\hat{\Psi}_N}{\partial t}=\Delta_{\mathbf{y}}\hat{\Psi}_N-\left(\frac{\mathrm{Pe}^2}{2}\left(\sum_{j=1}^N u\left(y_j\right)k_j\right)^2+|\mathbf{k}|^2\right)\hat{\Psi}_N,$$
$$\hat{\Psi}_N(\mathbf{k},\mathbf{y},0)=\prod_{j=1}^N\hat{T}_0(k_j,y_j),\quad\left.\frac{\partial\hat{\Psi}_N}{\partial y_j}\right|_{y_j=0,1}=0,\quad\forall\,1\le j\le N, \tag{6}$$

for (4), and yields

$$\frac{\partial\hat{\psi}_N}{\partial t}-\mathrm{iPe}\sqrt{\gamma}z\sum_{j=1}^N k_j u(y_j)\hat{\psi}_N+\gamma z\frac{\partial\hat{\psi}_N}{\partial z}=\Delta_{\mathbf{y}}\hat{\psi}_N-|\mathbf{k}|^2\hat{\psi}_N+\frac{\gamma}{2}\frac{\partial^2\hat{\psi}_N}{\partial z^2},$$
$$\hat{\psi}_N(\mathbf{k},\mathbf{y},z,0)=\prod_{j=1}^N\hat{T}_0(k_j,y_j),\quad\left.\frac{\partial\hat{\psi}_N}{\partial y_j}\right|_{y_j=0,1}=0,\quad\forall\,1\le j\le N, \tag{7}$$

for (5), where $\Delta_{\mathbf{y}}=\sum_{j=1}^N\frac{\partial^2}{\partial y_j^2}$. According to spectral theory of parabolic differential operators, the solution of (6) and (7) has an eigenfunction expansion

$$\hat{\Psi}_N(\mathbf{k},\mathbf{y},t)=\sum_{l=0}^\infty\beta_{N,l}(\mathbf{k})\phi_{N,l}(\mathbf{k},\mathbf{y})e^{-\lambda_{N,l}(\mathbf{k})t}. \tag{8}$$

When the statistics of velocity field is white in time, $\lambda_{N,l}$, $\phi_{N,l}$ are the eigenvalues and eigenfunctions of the eigenvalue problem

$$-\lambda_{N,l}\phi_{N,l}=\Delta_{\mathbf{y}}\phi_{N,l}-\left(\frac{\mathrm{Pe}^2}{2}\left(\sum_{j=1}^N u\left(y_j\right)k_j\right)^2+|\mathbf{k}|^2\right)\phi_{N,l},$$
$$\left.\frac{\partial\phi_{N,l}}{\partial y_j}\right|_{y_j=0,1}=0,\quad\forall\,1\le j\le N. \tag{9}$$

For simplicity, we scale $\phi_{N,l}$ so that $\{\phi_{N,l}\}_{l=0}^\infty$ form an orthonormal basis with respect to the inner product $\langle f(\mathbf{y}),g(\mathbf{y})\rangle=\int_{[0,1]^N}\mathrm{d}\mathbf{y}\,f(\mathbf{y})g(\mathbf{y})$ for all $\mathbf{k}$. $\beta_{N,l}$ are determined by the initial condition and the eigenfunction via $\beta_{N,l}(\mathbf{k})=\left\langle\prod_{j=1}^N\hat{T}_0(k_j,y_j),\phi_{N,l}(\mathbf{k},\mathbf{y})\right\rangle$. When $\xi(t)$ is the stationary Ornstein–Uhlenbeck process, $\phi_{N,l}(\mathbf{k},\mathbf{y})=\frac{1}{\sqrt{\pi}}\int_{-\infty}^{+\infty}\mathrm{d}z\varphi_{N,l}(\mathbf{k},\mathbf{y},z)e^{-z^2}$, where $\lambda_{N,l}$, $\varphi_{N,l}$ are the eigenvalues

and eigenfunctions of the eigenvalue problem

$$-\lambda_{N,l}\varphi_{N,l} = \mathrm{iPe}\sqrt{\gamma}z\sum_{j=1}^{N} k_i u(y_i)\varphi_{N,l} - \gamma z\frac{\partial\varphi_{N,l}}{\partial z} + \Delta_{\mathbf{y}}\varphi_{N,l}$$
$$-|\mathbf{k}|^2\varphi_{N,l} + \frac{\gamma}{2}\frac{\partial^2\varphi_{N,l}}{\partial z^2}, \quad \left.\frac{\partial\varphi_{N,l}}{\partial y_j}\right|_{y_j=0,1} = 0, \quad \forall 1\le j\le N. \tag{10}$$

We also choose $\varphi_{N,l}$ such that $\{\varphi_{N,l}\}_{l=0}^{\infty}$ form an orthonormal basis with respect to the inner product $\langle f(\mathbf{y},z), g(\mathbf{y},z)\rangle = \frac{1}{\sqrt{\pi}}\int_{-\infty}^{+\infty} dz \int_{[0,1]^N} d\mathbf{y} f(\mathbf{y},z)g^*(\mathbf{y},z)e^{-z^2}$ respectively, where g^* is the complex conjugate of g. $\beta_{N,l}$ have the same definition as the Gaussian white noise case.

Bronski and McLaughlin [18] proved that $\lambda_{N,l}(\mathbf{k})$ strictly increases with respect to the subscript l for all $\mathbf{k}$ and have a global minimum value at $\mathbf{k}=\mathbf{0}$, in particular, $\lambda_{N,0}(\mathbf{0})=0$, $\lambda_{N,1}(\mathbf{0})=\pi^2$. As a consequence, the series given in (8) is dominated at long times by the ground state $j=0$, since the other terms are $\mathcal{O}(e^{-\pi^2 t})$. This observation yields the following asymptotic formula valid at long times for arbitrary N-point correlation function of the scalar field

$$\Psi_N(\mathbf{x},\mathbf{y},t) = (2\pi)^{-\frac{N}{2}}\int_{\mathbb{R}^N} d\mathbf{k} e^{\mathrm{i}(\mathbf{x}\cdot\mathbf{k})}\beta_{N,0}(\mathbf{k})\phi_{N,0}(\mathbf{k},\mathbf{y})e^{-\lambda_{N,0}(\mathbf{k})t} + \mathcal{O}(e^{-\pi^2 t}), \quad t\to\infty. \tag{11}$$

This is an N-dimensional Laplace type integral with respect to the wavenumber $\mathbf{k}$. By formula (1) given in [33], the asymptotic expansion of $\Psi_N(\mathbf{x},\mathbf{y},t)$ for large t is

$$\Psi_N(\mathbf{x},\mathbf{y},t) = (2\pi t)^{-\frac{N}{2}}\det(\mathbf{\Lambda}_N)^{-1}\exp\left(-\frac{1}{2}\mathbf{x}\mathbf{\Lambda}_N^{-1}\mathbf{x}^{\mathrm{T}}\right) + \mathcal{O}(t^{-\frac{N+2}{2}}), \quad t\to\infty, \tag{12}$$

where $(\mathbf{\Lambda}_N)_{i,j} = \frac{\partial^2}{\partial k_i\partial k_j}\lambda_{N,0}(\mathbf{k})|_{\mathbf{k}=\mathbf{0}}$ is the Hessian matrix of the eigenvalue $\lambda_{N,0}(\mathbf{k})$ at $\mathbf{k}=\mathbf{0}$. An interesting observation from (12) is that Ψ_N satisfies a diffusion equation with the effective diffusion tensor $\mathbf{\Lambda}_N$ at long times,

$$\frac{\partial\Psi_N}{\partial t} = \nabla_{\mathbf{x}}\cdot(\mathbf{\Lambda}_N\nabla_{\mathbf{x}}\Psi_N). \tag{13}$$

If we interpret (4) or (5) as a Fokker–Planck equation for an N-particle system, (13) implies that the particles move like a non-standard N dimensional Brownian motion at long times.

The Hessian matrix $\mathbf{\Lambda}_N$ can be obtained by the perturbation method introduced in the appendix of [18]. We can utilize two properties of the eigenvalue problems described in (9) and (10) to simplify the calculation of $\mathbf{\Lambda}_N$. First, the eigenvalue problems are invariant under the permutation of wavenumbers $\mathbf{k}$, which implies $\frac{\partial^2}{\partial k_{i_1}\partial k_{j_1}}\lambda_{N,0}(\mathbf{k})|_{\mathbf{k}=\mathbf{0}} = \frac{\partial^2}{\partial k_{i_2}\partial k_{j_2}}\lambda_{N,0}(\mathbf{k})|_{\mathbf{k}=\mathbf{0}}$ for all $i_1\neq j_1, i_2\neq j_2$ and $\frac{\partial^2}{\partial k_i^2}\lambda_{N,0}(\mathbf{k})|_{\mathbf{k}=\mathbf{0}} = \frac{\partial^2}{\partial k_j^2}\lambda_{N,0}(\mathbf{k})|_{\mathbf{k}=\mathbf{0}}$ for all $1\le i,j\le N$. Second, in the N-dimensional eigenvalue problem, the eigenfunction associated with $\lambda_{N,0}$ is independent of y_N when $k_N=0$. In other words, the N dimensional eigenvalue problem can be reduced to $N-1$ dimensional eigenvalue problem by setting $k_N=0$. Based on these two properties, $\mathbf{\Lambda}_N$ only depends on the derivative of eigenvalues in the one-dimensional eigenvalue problem $\lambda^{(2)} = \frac{\partial^2}{\partial k_1^2}\lambda_{1,0}(k_1)|_{k_1=0}$ and the derivative of eigenvalues in the two-dimensional eigenvalue problem $\lambda^{(1,1)} = \frac{\partial^2}{\partial k_1\partial k_2}\lambda_{2,0}(k_1,k_2)|_{k_1=0,k_2=0}$.

Here, we are primarily concerned with single-point statistics, namely the moment of the random scalar field at point (x,y), $\langle T^N(x,y,t)\rangle_{\xi(t)} = \Psi_N(\mathbf{x},\mathbf{y},t)$, where all components of $\mathbf{x},\mathbf{y}$ are x,y, namely $x=x_1=x_2=\cdots=x_N$, $y=y_1=y_2=\cdots=y_N$. Hence, as $t\to\infty$, the first three moments are

$$\begin{aligned}
\langle T(x,y,t)\rangle_{\xi(t)} &= \frac{1}{(2\pi t)^{\frac{1}{2}}\sqrt{\lambda^{(2)}}} + \mathcal{O}(t^{-\frac{3}{2}}),\\
\langle T^2(x,y,t)\rangle_{\xi(t)} &= \frac{1}{2\pi t\sqrt{(\lambda^{(2)})^2-(\lambda^{(1,1)})^2}} + \mathcal{O}(t^{-2}),\\
\langle T^3(x,y,t)\rangle_{\xi(t)} &= \frac{1}{(2\pi t)^{\frac{3}{2}}\sqrt{(\lambda^{(2)}-\lambda^{(1,1)})^2(\lambda^{(2)}+2\lambda^{(1,1)})}} + \mathcal{O}(t^{-\frac{5}{2}}).
\end{aligned} \tag{14}$$

Here, we emphasize that the denominator in (14) is the determinant of the diffusion tensor $\mathbf{\Lambda}_N$. When $\xi(t)$ is a Gaussian white noise process, the derivatives of eigenvalues in (14) are

$$\lambda^{(2)} = 2+\mathrm{Pe}^2\int^1 dy\, u^2(y), \quad \lambda^{(1,1)} = \mathrm{Pe}^2\left(\int_0^1 dy\, u(y)\right)^2 = \mathrm{Pe}^2\bar{u}^2. \tag{15}$$

Additionally, when $\xi(t)$ is the stationary Ornstein–Uhlenbeck process, the derivatives of eigenvalues in (14) are

$$\lambda^{(2)} = 2+\mathrm{Pe}^2\sqrt{\gamma}\int_0^1 dy\, u(y)\left\{\frac{\cosh\left(\sqrt{\gamma}y\right)}{\sinh\left(\sqrt{\gamma}\right)}\int_0^1 ds\, u(s)\cosh\left(\sqrt{\gamma}\,(1-s)\right) - \int_0^y ds\, u(s)\sinh\left(\sqrt{\gamma}(y-s)\right)\right\}, \tag{16}$$
$$\lambda^{(1,1)} = \mathrm{Pe}^2\bar{u}^2.$$

The white noise can be regraded as a limiting case of vanishing correlation time γ^{-1} in the stationary Ornstein–Uhlenbeck process. It is natural to ask whether the scalar field statistics with $\xi(t)$ an Ornstein–Uhlenbeck process asymptotically satisfies, as $\gamma\to\infty$, the corresponding model with white noise process. In the free-space problem, Resnick [22] proves this for linear shear flow $u(y)=y$ via the exact formula of Ψ_N. In channel domain problem, the asymptotic analysis shows that (16) converges to (15) as $\gamma\to+\infty$, which supports this compatibility for large values of the parameter γ. In the free space problem, Vanden-Eijnden [23] proved that both of the two flows we considered in this paper share the same limiting distribution of the scalar field at long times for any γ. However, in channel domains, the differences between (15) and (16) lead to different corresponding limiting distributions. Thus, impermeable boundaries can affect the limiting distribution of the random scalar fields.

The right hand side of (12) is independent of x,y, which means all points in the domain have the same statistics behavior at long times. Without loss of generality, we focus on the single point $T(0,0,t)$ of the random scalar field. In [28], the authors derived the PDF of $T(0,0,t)$ at long times for the free space version of (3) and $u(y)=y$, $\mathrm{Pe}=1$ using the method of characteristics and the Green's function. The study of the explicit formula of PDF for the free space problem shows that the skewness of the PDF for $T(0,0,t)$ is positive at long times while the numerical studies show the skewness becomes negative in presence of impermeable channel boundaries, demonstrating how the impermeable boundary has a crucial impact on the PDF of random scalar flied. With the long time asymptotic expansion of moments provided in (14), we can theoretically study the skewness of $T(0,0,t)$ for various parameters and more general shear flows.

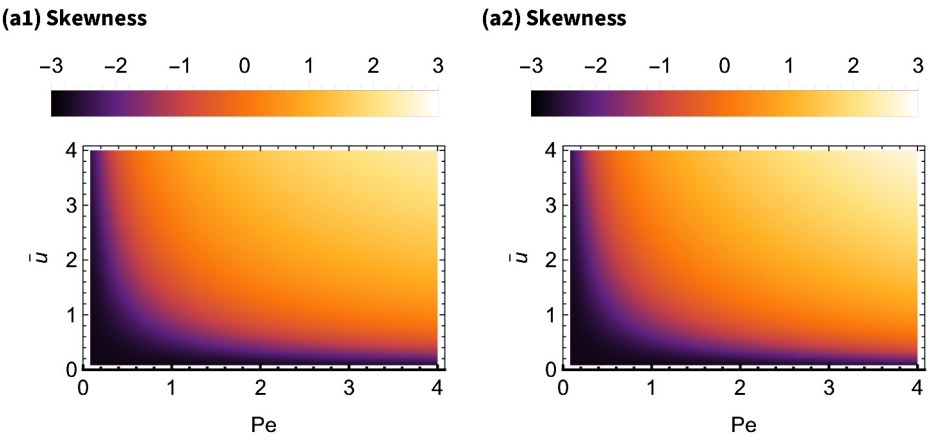

Fig. 1. The skewness limit of $T(0,0,t)$ at long times for various Péclet numbers and $\bar{u}$. In both panels, the flow takes the form $\mathrm{Pe}\,u(y)\xi(t)$, where $u(y)=(y+A)$ and $\bar{u}=A-\frac{1}{2}$. In panel (a1), $\xi(t)$ is the Gaussian white noise process. In panel (a2), $\xi(t)$ is the stationary Ornstein–Uhlenbeck process with $\gamma=1$.

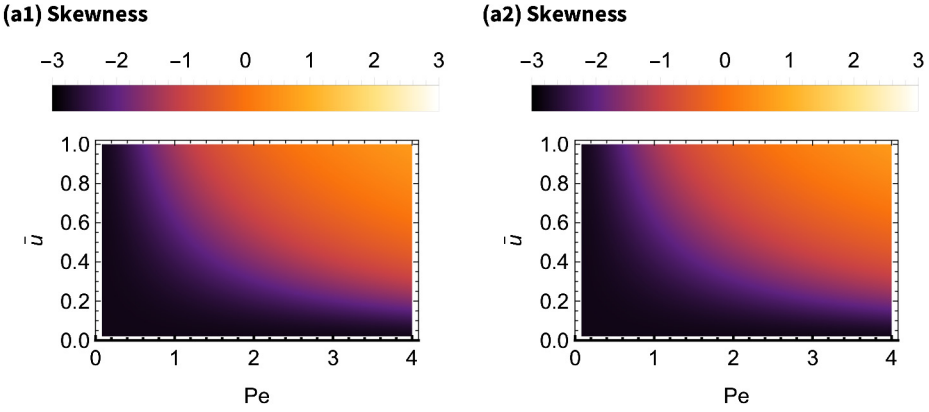

Fig. 2. The skewness limit of $T(0,0,t)$ at long times for various Péclet numbers and $\bar{u}$. In both panels, the flow takes the form $\mathrm{Pe}u(y)\xi(t)$, where $u(y)=\theta(a-y)$ (with θ denoting the Heaviside step function) and $\bar{u}=a$. In panel (a1), $\xi(t)$ is the Gaussian white noise process. In panel (a2), $\xi(t)$ is the stationary Ornstein–Uhlenbeck process with $\gamma=1$.

Based on (14), as $t\to\infty$, the variance of $T(x,y,t)$ is given by

$$\mathrm{Var}(T)=\left\langle (T-\langle T\rangle)^2\right\rangle=\left(\frac{1}{\sqrt{(\lambda^{(2)})^2-(\lambda^{(1,1)})^2}}-\frac{1}{\lambda^{(2)}}\right)\frac{1}{2\pi t}+\mathcal{O}(t^{-2}). \tag{17}$$

Notice that coefficient of t^{-1} in (17) is strictly positive if $\lambda^{(1,1)}\neq 0$, which requires $\bar{u}\neq 0$. As $t\to\infty$, the skewness of $T(x,y,t)$ has the following asymptotic expansion

$$\begin{aligned}\mathrm{S}(T)&=\frac{\left\langle (T-\langle T\rangle)^3\right\rangle}{(\mathrm{Var}(T))^{\frac{3}{2}}}\\&=\frac{\dfrac{1}{\sqrt{(\lambda^{(2)}-\lambda^{(1,1)})^2(\lambda^{(2)}+2\lambda^{(1,1)})}}-\dfrac{3}{\sqrt{\lambda^{(2)}\left((\lambda^{(2)})^2-(\lambda^{(1,1)})^2\right)}}+\dfrac{2}{(\lambda^{(2)})^{\frac{3}{2}}}}{\left(\dfrac{1}{\sqrt{(\lambda^{(2)})^2-(\lambda^{(1,1)})^2}}-\dfrac{1}{\lambda^{(2)}}\right)^{\frac{3}{2}}}\\&\quad+\mathcal{O}(t^{-1}).\end{aligned} \tag{18}$$

The first term on the right hand side of (18) shows the existence of the long time limit of skewness, which means the PDF of $T(0,0,t)$ has a persisting asymmetry. There are five factors that affect the limit value: the Péclet number Pe, the mean of spatial component of flow $\bar{u}$, the shape of $u(y)$, the temporal fluctuation $\xi(t)$ and the OU damping parameter γ.

Fig. 1 and Fig. 2 show the long time limit of skewness of $T(0,0,t)$ for the flow with $u(y)=y+A$ and $u(y)=\theta(a-y)$ (with θ denoting the Heaviside step function) for various Péclet numbers and $\bar{u}$, respectively. Panel (a1) in Fig. 1 shows that the skewness limit is negative when $\bar{u}=1/2$, $\mathrm{Pe}=1$, which is consistent with Monte-Carlo simulation results reported in [28]. Both of those figures have a similar pattern. The skewness is negative when Pe or $\bar{u}$ is small and positive when they are large. In an attempt to rigorously demonstrate our conclusion for any $u(y)$ at long times, we derive the leading order asymptotic expansion at low Péclet number from (18), thereby, we obtain

$$S(T)=-2\sqrt{2}+\frac{9\mathrm{Pe}^2\bar{u}^2}{\sqrt{2}}+\mathcal{O}(\mathrm{Pe}^4),\quad \mathrm{Pe}\to 0,\quad t\to\infty. \tag{19}$$

Subsequently, we observe from (19) that the long time limit of skewness is negative at low Péclet numbers (equivalently, for sufficiently small spatial mean of the flow denoted by $\bar{u}$). In particular, in the zero Péclet number limit, the skewness becomes $-2\sqrt{2}$. Alternatively, with the step function shear flow, the differences are larger as can be seen by comparing panel (a1) or panel (a2) in Fig. 1 with the corresponding panels in Fig. 2. One can see that the change of $u(y)$ dramatically changes the long time asymptotics of the skewness in its $\mathrm{Pe}-\bar{u}$ dependence. Of course, while the Ornstein–Uhlenbeck process yields different numerical values compared with the white noise process, for the parameter

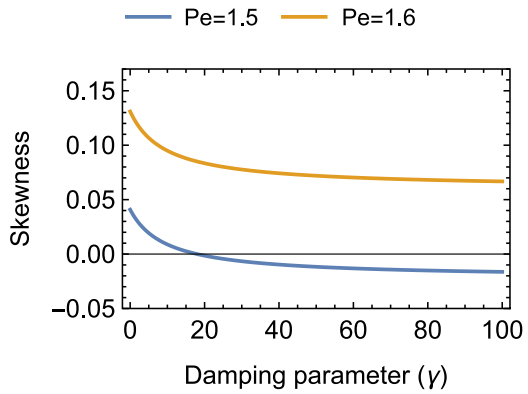

Fig. 3. The skewness limit of $T(0,0,t)$ at long times for various damping parameters γ. The flow is $\mathrm{Pe}(y+1.2)\xi(t)$, where $\xi(t)$ is a stationary Ornstein–Uhlenbeck process with the damping parameter γ. The cases of Pe = 1.5 and Pe = 1.6 are shown by the blue and orange curves, respectively. (For interpretation of the references to color in this figure legend, the reader is referred to the web version of this article.)

region $(\mathrm{Pe}, \bar{u}) \in [0,4]\times[0,4]$ shown in the figures the relative difference between them is less than 0.1. Hence it is hard to observe a difference when comparing the left and right panels of Fig. 1 and Fig. 2 respectively.

In Fig. 3, we show the dependence of the skewness long time limit on the damping parameter γ. Note that depending on Pe and $u(y)$, the sign of skewness can be made to change by varying γ.

We also implement the backward Monte-Carlo method described in Appendix A.1 to verify the long-time asymptotic analysis results by numerical simulations. We simulate $T(0,0,t)$ with the initial condition $T_0(x,y) = e^{-x^2}/\sqrt{\pi}$ for different flows, and results are shown in Fig. 4. The blue curves are the numerical results of skewness evolution and the green horizontal lines are the skewness limits computed by (18). The consistency between them validates (18). In panels (a1) and (a2), $\xi(t)$ is white noise process, $u(y)$ are y and $y+1/2$ respectively. One can see that the larger spatial mean of the flow leads to longer transient dynamics before reaching the long time asymptotic state. In panels (b1) and (b2), $\xi(t)$ is the stationary Ornstein–Uhlenbeck process and $u(y) = y$, the damping parameters γ are 5 and 50, respectively. Comparison between panels (b1) and (b2) shows the longer correlation time in the panel (b1) yields a more dramatic transient dynamics in the skewness evolution. Comparing the panels $(a1)$ and $(b2)$, when the correlation time γ^{-1} is small, we observe the convergence of the Ornstein–Uhlenbeck case to the white noise case.

4. An explicit example for scalar intermittency

In this section we study a special case of (1), which yields an exact formula valid at all times. Therefore, this is a solid benchmark for the long time asymptotic analysis derived in the previous section. In [27], the authors call the advection–diffusion equation formulated in (1) with $u(y) = 1$ the "wind model". They study the one dimensional problem when $\xi(t)$ is the Gaussian white noise process. Here, we present the exact formula of N-point correlation function Ψ_N for the channel domain problem with any general Gaussian process $\xi(t)$.

The associated Green's function $G(x,y,x_0,y_0,t)$, that is, the solution of (1) with the initial condition $T(x,y,0) = \delta(x-x_0)\delta(y-y_0)$, can be obtained by the separation of variables and the method of characteristics (for basics of these methods see [34]),

$$G(x,y,x_0,y_0,t) = K(y,y_0,t)\frac{1}{\sqrt{4\pi t}}\exp\left(-\frac{(x-x_0-\mathrm{Pe}\int_0^t \mathrm{d}s\,\xi(s))^2}{4t}\right), \tag{20}$$

where $K(y,y_0,t) = 1 + 2\sum_{n=1}^{\infty}\cos(n\pi y)\cos(n\pi y_0)\exp(-n^2\pi^2 t)$ is the heat kernel on the interval $[0,1]$. The solution with general initial condition $T_0(x,y)$ can be constructed by the Green function via convolution,

$$T(x,y,t) = \int_{-\infty}^{+\infty}\mathrm{d}x_0\int_0^1 \mathrm{d}y_0 T_0(x_0,y_0)G(x,y,x_0,y_0,t). \tag{21}$$

By the definition of Ψ_N and Fourier transform, we have

$$\begin{aligned}&\Psi_N(\mathbf{x},\mathbf{y},t) = \\ &\int_{\mathbb{R}^N}\mathrm{d}\mathbf{x}_0\int_{[0,1]^N}\mathrm{d}\mathbf{y}_0\frac{1}{(2\pi)^N}\int_{\mathbb{R}^N}\mathrm{d}\mathbf{k}\exp\left(\sum_{j=1}^N \mathrm{i}k_j(x_j-x_{0j}) - tk_j^2\right)\\ &\times\left\langle\exp(-\mathrm{iPe}\sum_{j=1}^N k_j\int_0^t \mathrm{d}s\xi(s))\right\rangle\times\prod_{j=1}^N K(y_j,y_{0j},t)T_0(x_{0j},y_{0j}),\end{aligned} \tag{22}$$

where $\mathbf{x}_0 = (x_{01},x_{02},\ldots,x_{0N})$, $\mathbf{y}_0 = (y_{01},y_{02},\ldots,y_{0N})$. Since $\xi(t)$ is a Gaussian process, $\int_0^t \mathrm{d}s\xi(s)$ is a normal random variable at any time instant. By utilizing the characteristic function of normal random variable, we obtain:

$$\begin{aligned}&\Psi_N(\mathbf{x},\mathbf{y},t) = \\ &\int_{\mathbb{R}^N}\mathrm{d}\mathbf{x}_0\int_{[0,1]^N}\mathrm{d}\mathbf{y}_0\frac{1}{(2\pi)^N}\int_{\mathbb{R}^N}\mathrm{d}\mathbf{k}\exp\left(\sum_{j=1}^N \mathrm{i}k_j(x_j-x_{0j}) - tk_j^2\right)\\ &\exp\left(-\tfrac{1}{2}\sigma(t)\left(\mathrm{Pe}\sum_{j=1}^N k_j\right)^2\right)\times\prod_{j=1}^N K(y_j,y_{0j},t)T_0(x_{0j},y_{0j}),\end{aligned} \tag{23}$$

where $\sigma(t)$ is the variance of stochastic process $\int_0^t \mathrm{d}s\xi(s)$. $\sigma(t) = t$ when $\xi(t)$ is the Gaussian white noise process, $\sigma(t) = t + \frac{e^{-\gamma t}-1}{\gamma}$ when $\xi(t)$ is the OU process. Comparing this integral with the multivariate normal distribution, we have

$$\begin{aligned}\Psi_N(\mathbf{x},\mathbf{y},t) = &\int_{\mathbb{R}^N}\mathrm{d}\mathbf{x}_0\int_{[0,1]^N}\mathrm{d}\mathbf{y}_0\frac{\exp\left(-\frac{1}{2}(\mathbf{x}-\mathbf{x}_0)\Lambda^{-1}(\mathbf{x}-\mathbf{x}_0)^{\mathrm{T}}\right)}{(2\pi)^{\frac{N}{2}}\sqrt{\det(\Lambda)}}\\ &\times\prod_{j=1}^N K(y_j,y_{0j},t)T_0(x_{0j},y_{0j}),\end{aligned} \tag{24}$$

where $\Lambda = 2tI + \sigma(t)\mathrm{Pe}^2\mathbf{e}^{\mathrm{T}}\mathbf{e}$, I is the identity matrix of size $N\times N$ and $\mathbf{e}$ is a $1\times N$ vector with 1 in all coordinate. By the Sherman–Morrison formula [35], $\Lambda^{-1} = (2t)^{-1}\left(I - \frac{\sigma(t)\mathrm{Pe}^2\mathbf{e}^{\mathrm{T}}\mathbf{e}}{2t+N\sigma(t)\mathrm{Pe}^2}\right)$, and by the matrix determinant lemma, $\det(\Lambda) = (2t)^N\left(1+\frac{N\sigma(t)\mathrm{Pe}^2}{2t}\right)$. To compare with the Nth moment $\langle T^N(x,y,t)\rangle$, we choose the initial condition as $T_0(x,y) = \delta(x)$. Hence, the solution is independent of y,

$$T(x,t) = \frac{1}{\sqrt{4\pi t}}\exp\left(-\frac{\left(x-\mathrm{Pe}\int_0^t \mathrm{d}s\xi(s)\right)^2}{4t}\right), \tag{25}$$

and the Nth moment is

$$\langle T^N(x,t)\rangle = \frac{(4\pi t)^{-\frac{N}{2}}}{\sqrt{1+\frac{N\sigma(t)\mathrm{Pe}^2}{2t}}}\exp\left(-\frac{Nx^2}{4t}\left(1-\frac{N\mathrm{Pe}^2\sigma(t)}{N\mathrm{Pe}^2\sigma(t)+2t}\right)\right).$$

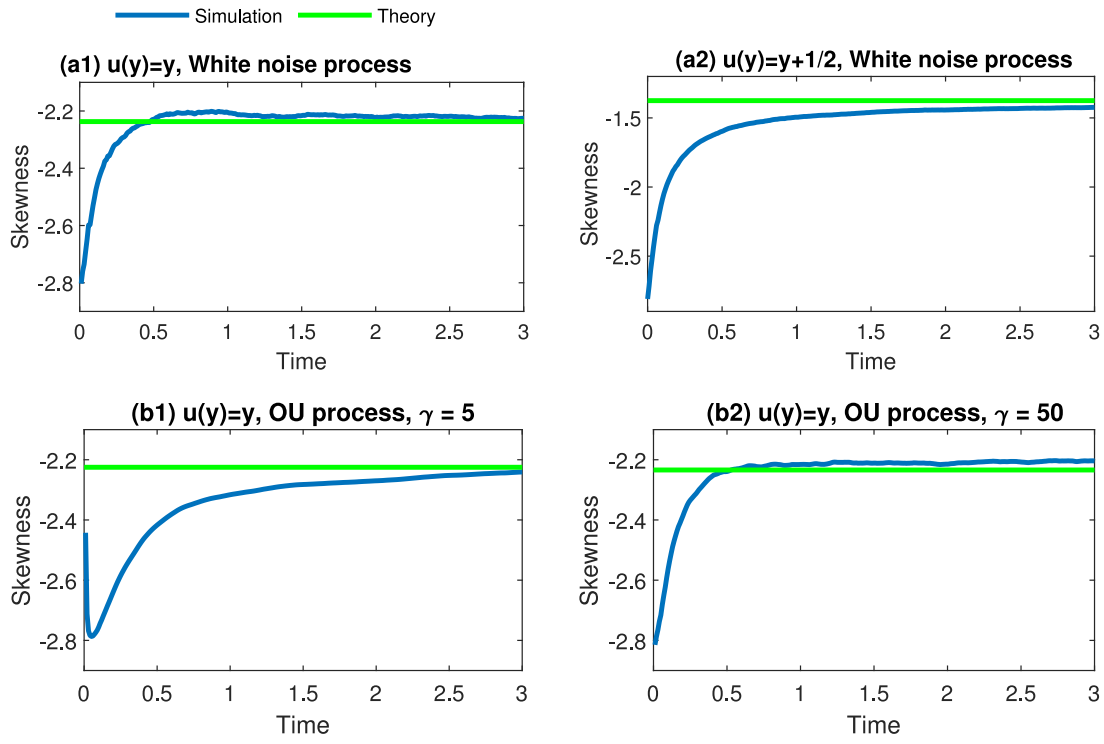

Fig. 4. Skewness evolution for random shear flows fluctuating with Gaussian white noise and Ornstein–Uhlenbeck process statistics. Here, we provide the skewness evolution for random shear flows with different spatial means and different fluctuation statistics obtained from Monte Carlo simulations along with the long time asymptotics theoretical predictions of skewness (18). In panels (a1)–(a2) we provide the skewness evolution and corresponding long time asymptotics for flows with Gaussian white noise fluctuations. Next, in panels (b1)–(b2), we provide the skewness evolution and its long time asymptotics for random shear flow $u(y) = y$ with fluctuations that has Ornstein–Uhlenbeck process statistics. Furthermore, in panels (b1) and (b2), the correlation strength parameter of Ornstein–Uhlenbeck processes is $\gamma = 5$ and $\gamma = 50$, respectively. In all panels, Monte Carlo simulation results are shown in blue curves where the theoretical predictions of the long time limits of skewness are shown in green horizontal lines. (For interpretation of the references to color in this figure legend, the reader is referred to the web version of this article.)

(26)

The long time asymptotic expansion of (26) is consistent with (14). We compute the skewness evolution of the scalar field at the point $(0, 0)$ for various Péclet numbers by (26) and present the results in Fig. 5. Panel (a1) shows that, with the line source initial data and Gaussian white noise process $\xi(t)$, the skewness is a constant for all time. In contrast, panel (a2) shows that the finite correlation in OU process $\xi(t)$ introduces a noticeable transient before reaching the long time asymptotic state. This phenomenon weakens as the Péclet number increases.

With the exact formula of N-point correlation function, we can study the multi-point statistics of the random scalar field. Let us consider the average of the scalar field over $x \in [-a, a]$,

$$M(a,t) = \frac{1}{2a}\int_{-a}^{a} T(x,t)\mathrm{d}x = \frac{1}{2a}\left(\mathrm{erf}\left(\frac{a+\mathrm{Pe}\int_0^t \mathrm{d}s\xi(s)}{2\sqrt{t}}\right) + \mathrm{erf}\left(\frac{a-\mathrm{Pe}\int_0^t \mathrm{d}s\xi(s)}{2\sqrt{t}}\right)\right), \tag{27}$$

where $\mathrm{erf}(z) = \frac{2}{\sqrt{\pi}}\int_0^z \mathrm{d}te^{-t^2}$ is the error function. When $a \to 0$, $M(a, t)$ will converge to $T(0, t)$.

By switching the order of integration and ensemble average, the Nth moment of $M(a, t)$ is

$$\left\langle M(a,t)^N\right\rangle_{\xi(t)} = (2a)^{-N}\int_{[-a,a]^N}\mathrm{d}\mathbf{x}\left\langle\prod_{j=1}^{N} T(x_j,t)\right\rangle_{\xi(t)}. \tag{28}$$

Fig. 6 shows the skewness evolution of $M(1/10, t)$ computed by (28) for various Péclet numbers and temporal fluctuations obeying different statistics, in particular, Gaussian-white noise and Ornstein–Uhlenbeck processes statistics. The overall behavior of the skewness of $M(1/10, t)$ is strikingly similar to the skewness of $T(0, 0, t)$ presented in Fig. 5. However, there is a very subtle difference between them at the earlier stage which cannot be seen in Fig. 6. To show this subtle difference, we plot the skewness of $M(1/10, t)$ in panel (a2) of Fig. 7 when $\mathrm{Pe} = 1$ and $\xi(t)$ is the white noise process. Unlike the skewness of $T(0, 0, t)$ which is a constant for all time, we see the skewness of $M(1/10, t)$ starts from a lower value due to the spatial correlation of the random scalar field $T(x, y, t)$. As a result of the diffusion, all $T(x, y, t)$ over the region $(x, y) \in [-1/10, 1/10] \times [0, 1]$ converges to the same value at long times. As shown in panel (a2) of Fig. 7, the skewness of $M(1/10, t)$ converges to the skewness of $T(0, t)$ at diffusion time scale.

To verify our theoretical analysis, we compute the skewness by the Direct Monte-Carlo (DMC) method proposed in [28] and plot the results as green circles in panel (a2) of Fig. 7. The consistency of the two approaches demonstrates the validity of the theoretical analysis in this section. Panel (a1) in Fig. 7 depicts the PDF of $M(1/10, 1)$ obtained by DMC method for different Péclet numbers. It shows that with increasing Péclet number the PDF changes from negatively-skewed to positively-skewed, which is consistent with the observation we made from Figs. 5 and 6.

5. Conclusion

We have demonstrated analytically and numerically that the single point statistics, in particular *skewness*, of a passive scalar advected by a random shear flow with deterministic initial data have opposite symmetric behaviors at long times depending on

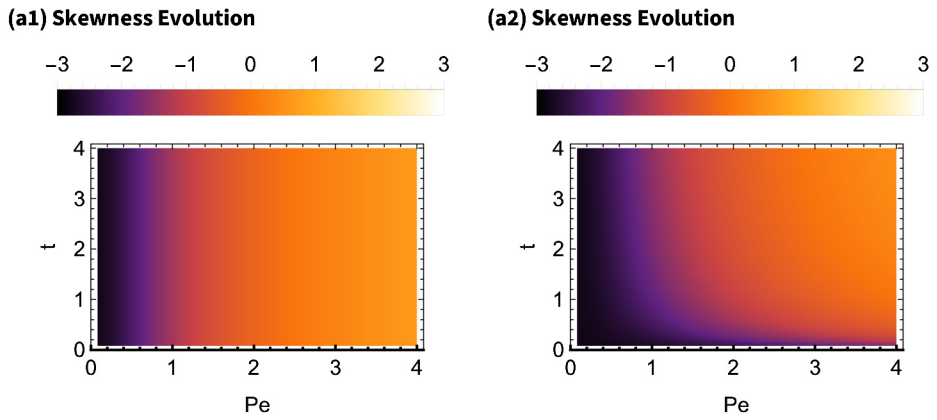

Fig. 5. Evolution of the random variable $T(0, 0, t)$ for various Péclet numbers and time. In both panels, the flow takes the form $\mathrm{Pe}u(y)\xi(t)$, where $u(y) = 1$ and $\bar{u} = 1$. In panel (a1), $\xi(t)$ is the Gaussian white noise process. In panel (a2), $\xi(t)$ is the stationary Ornstein–Uhlenbeck process with $\gamma = 1$.

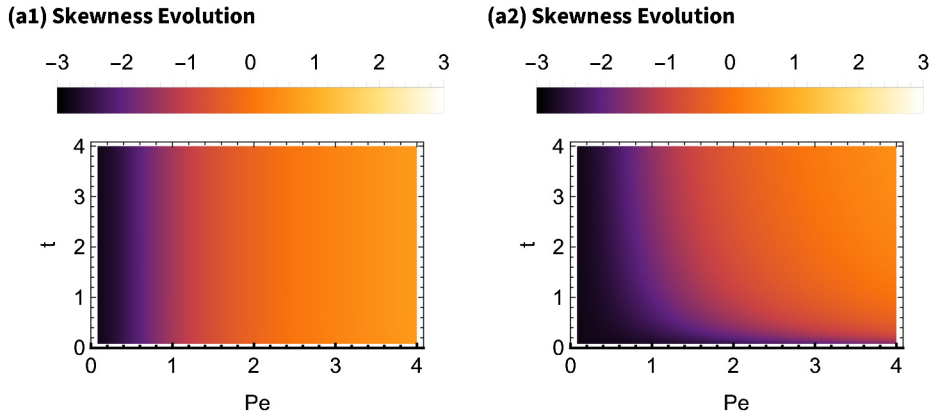

Fig. 6. Evolution of the spatially averaged random variable $M(\frac{1}{10}, t)$ defined in (27) for various Péclet numbers and time. In both panels, the flow takes the form $\mathrm{Pe}u(y)\xi(t)$, where $u(y) = 1$ and $\bar{u} = 1$. In panel (a1), $\xi(t)$ is the Gaussian white noise process. In panel (a2), $\xi(t)$ is the stationary Ornstein–Uhlenbeck process with $\gamma = 1$. .

the presence or the absence of *impermeable boundaries* . We have investigated two types of flow temporal fluctuations, respectively modeled by Gaussian white noise and stationary Ornstein–Uhlenbeck processes. We have shown the convergence of the Ornstein–Uhlenbeck case to its white noise counterpart in the limit $\gamma \to \infty$ of the OU damping parameter, which generalizes the conclusion in the article [22] for free space to the confined channel domain problem. Importantly, we observe that the OU damping parameter γ plays a more significant role in channel domains than in the free space problem. The first three moments of the scalar distribution at infinite time depend on the correlation time γ^{-1} in the channel domain, which is in strong contrast to the result of Vanden-Eijnden [23] in free space where the PDF at long time is independent of γ. We have presented the detailed discussions of three different shear flows. All of them show the transient of skewness from negative to positive when increasing either the Péclet number or $\bar{u}$, which rigorizes and generalizes the observation from the simulation result in [28]. To find a benchmark for theoretical analysis, we have generalized the wind model studied in [27] and derived the exact formula of the N-point correlation function for the flow with no spatial dependence and Gaussian temporal fluctuation. The long time asymptotic expansion of this formula is consistent with our theory for general shear flows.

We have presented numerical studies that verify the validity of our theoretical results. For the wind model, we performed Direct Monte-Carlo simulation and observed that the Péclet number can adjust the time at which the skewness of the distribution changes sign. Due to the lack of an exact solution for general shear flows, we implemented backward Monte-Carlo simulations to verify the long time asymptotic results we derived. We confirmed that as the damping parameter γ increases the stationary Ornstein–Uhlenbeck case converges to the white noise case and found that transient for the skewness of the passive scalar's PDF to reach its long time asymptotic state lasts longer as the damping parameter decreases.

Future work will include considering an experimental campaign with the associated theoretical analysis. Our recent study [31] regarding the enhanced diffusion [29] and third spatial Aris moment [30] induced by a periodically moving wall led to the development of an experimental framework of the model explored in this paper. The computer controlled robotic arm we developed for the periodic study can be applied to the case of a randomly moving wall, such as the OU process $\xi(t)$, with suitable parameters. At large viscosity, the induced flow in the channel can be modeled by $y\xi(t)$. Hence, the concentration of tracers in the fluid satisfies the advection–diffusion equation provided in (1). The symmetry properties of the tracer's PDF can be predicted by the theory we developed here. Perhaps even more interesting will be considering cases in which the physical shear flow is not decomposed into a product of a function of

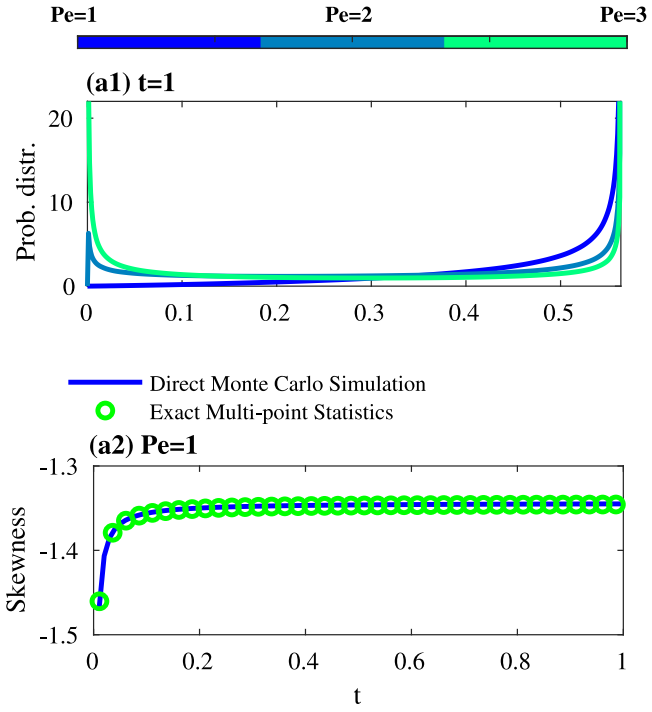

Fig. 7. Evolution of the spatially averaged random variable defined in (27) with the Gaussian white noise process $\xi(t)$ for various Péclet numbers and time. In panel (a1), we superposed 3 probability distributions of $M(1/10, 1)$ with Pe $= 1$ (blue), Pe $= 2$ (dark green) and Pe $= 3$ (green). Next, in panel (a2), we show the skewness of $M(1/10, t)$ calculated through the Direct Monte Carlo simulations (blue line) and the numerically integrating the formula (28) (green circle). (For interpretation of the references to color in this figure legend, the reader is referred to the web version of this article.)

space and a function of time, such as happens with the general nonlinear Stokes layer solutions at finite viscosities. Another interesting experimental configuration is the random tangential motion of a non-flat wall which generates random non-sheared motions in the fluid. Mercer and Roberts [36] derived the long time asymptotic approximations to the equation governing the longitudinal dispersion of a passive contaminant advected by a pressure driven flow in a channel with non-flat walls via the central manifold theory. Recently, [37–39] developed rigorous justifications of the application of central manifold approach on Taylor dispersion via spectral decomposition and hypocoercivity method. We expect those techniques used in the study of Taylor dispersion may well be extendable to the case of random flows in such geometries.

Although the leading order terms of N-point correlation function provide us rich information about the limiting distribution of the scalar field, there are still many interesting questions which need the knowledge of the higher order corrections of the N-point correlation function to answer. First, we use the assumption that initial data has the nonzero spatial mean $\int_{-\infty}^{\infty} dx \int_0^1 dy T_0(x, y) \neq 0$ in the nondimensionalization procedure. Once the spatial mean vanishes, the leading order terms in (14) vanish. In this case, we need the derivative of $\frac{\partial}{\partial k}\hat{T}_0(k, t)\Big|_{k=0}$ and the higher order derivatives of the eigenvalues and eigenfunctions to derive nontrivial asymptotic expansions of N-point correlation function. Second, the numerical simulation in Fig. 4 shows the dependence of the transient time scale on the correlation time of the OU process. We expect the higher order corrections can yield a rigorous prediction of the transient time scale. The last question concerns for the flow with a vanishing spatial mean. Such a case could be experimentally observed by having two walls executing equal but opposite parallel motions, or by putting the observer in an appropriate frame of reference. The asymptotic analysis strategy we presented does not technically fail if the spatial average of the flow in the physical domain vanishes, namely $\bar{u} = \int_0^1 dy u(y) = 0$, as the distribution is expected to be symmetric at long time in this case, consistent with our asymptotics which show that the third moment vanishes at long time with a zero spatial mean. However, the case with $\bar{u} = 0$ requires considerable additional analysis to investigate how the long time PDF relaxes to a symmetric state. To see that, it is easy to check that the coefficient of t^{-1} in (17) becomes zero as well as the coefficient of $t^{-\frac{3}{2}}$ and $t^{-\frac{5}{2}}$ in centered third moment expansion. That means the higher-order terms in (14) are needed for the analysis of skewness for the case $\bar{u} = 0$. Kilic's thesis work [40] reports preliminary results that the point statistics induced by some flows with $\bar{u} = 0$ have distinct behaviors from the case $\bar{u} \neq 0$. More detailed analysis in this direction has been completed and it will be reported separately.

Additional interesting directions worth exploring include considering how sourcing the passive scalar or studying a scalar with a mean gradient can modify our findings [41–43], as well as considering how flow possessing an energy cascade can lead to different scalings [44,45], or inherited scalar spectra [41]. Also, it is interesting to consider if there are more general initial configurations, e.g. [46] or different flow configurations as in [47] which can lead to different long time asymptotics than studied here.

CRediT authorship contribution statement

Roberto Camassa: Conceptualization, Methodology, Software, Validation, Formal analysis, Writing - original draft, Writing - review & editing. **Lingyun Ding:** Conceptualization, Methodology, Software, Validation, Formal analysis, Writing - original draft, Writing - review & editing. **Zeliha Kilic:** Conceptualization, Methodology, Software, Validation, Formal analysis, Writing - original draft, Writing - review & editing. **Richard M. McLaughlin:** Conceptualization, Methodology, Software, Validation, Formal analysis, Writing - original draft, Writing - review & editing.

Declaration of competing interest

The authors declare that they have no known competing financial interests or personal relationships that could have appeared to influence the work reported in this paper.

Acknowledgment

We acknowledge funding received from the following NSF Grant Nos. DMS-1517879, and DMS-1910824; and ONR ONR N00014-18-1-2490.

Appendix

A.1. Numerical simulations

To verify the long-time asymptotic analysis results, we need to simulate samples of random scalar field $T(x, y, t)$ at a single point (x, y). The Feynman–Kac formula based backward Monte-Carlo method is efficient in this case, since it can access the single point value of the scalar field without solving the global solution of (1). For each realization of the stochastic process $\xi(t)$, the random field has the path integral representation $T(x, y, t) = \langle T_0(X_t(t), Y_t(t))\rangle_{B_1(t),B_2(t)}$ by the Feynman–Kac formula, where

Table 1
Lists of abbreviations.

Full form	Abbreviation
Direct Monte-Carlo	DMC
Independent and identically distributed	i.i.d.
Ornstein–Uhlenbeck	OU
Partial differential equation	PDE
Probability distribution function	PDF
Stochastic differential equation	SDE

$X_t(s)$, $Y_t(s)$ are the solutions of the stochastic differential equation (SDE)

$$\begin{aligned} \mathrm{d}X_t(s) = -\mathrm{Pe}\xi(t-s)u(Y_t(s))\mathrm{d}s + \sqrt{2}\mathrm{d}B_1(s), \quad \mathrm{d}Y_t(s) = \sqrt{2}\mathrm{d}B_2(s), \\ X_t(0) = x, \quad Y_t(0) = y, \end{aligned} \tag{29}$$

where $B_i(s)$ are independent Brownian motions. To evaluate the path integral representation at a different time instant t_i, one needs to solve the SDE again with that new parameter t_i, which is expensive in practice. Notice that both the Gaussian white noise process and the stationary OU process is stationary and temporally homogeneous, so $\xi(t-s) = \xi(s)$ in the sense of distribution. This property allows us to solve a simpler but equivalent SDE,

$$\begin{aligned} \mathrm{d}X(s) = -\mathrm{Pe}\xi(s)u(Y(s))\mathrm{d}s + \sqrt{2}\mathrm{d}B_1(s), \quad \mathrm{d}Y(s) = \sqrt{2}\mathrm{d}B_2(s), \\ X(0) = x, \quad Y(0) = y. \end{aligned} \tag{30}$$

Since the solution is independent of the parameter t, we only need to solve this SDE once with the given realization of Brownian motions, which saves a lot of computation cost. We solve the SDE by the Euler scheme with a time increment $\Delta s = 0.01$ and uniform time nodes $s_{i+1} = s_i + \Delta s$,

$$\begin{aligned} X_{i+1} = X_i - \mathrm{Pe}\xi_i u(Y_i)\Delta s + \sqrt{2\Delta s}n_{1,i}, \quad Y_{i+1} = Y_i + \sqrt{2\Delta s}n_{2,i}, \\ X_0 = x, \quad Y_0 = y, \end{aligned} \tag{31}$$

where $X_i = X(s_i)$, $Y_i = Y(s_i)$, $\xi_i = \xi(s_i)$ are the appromation of stochastic processes at $s = s_i$. $n_{1,i}$, $n_{2,i}$ are standard independent and identically distributed (i.i.d.) normal random variables which are produced by the Mersenne Twister uniform random number generator and Marsaglia polar method [48]. We implement the impermeable boundary conditions by imposing billiard-like reflection rules on the boundary $y = 0, 1$. We typically generate 10^6 realization of $\xi(s)$. The realization of the Gaussian white noise process are produced by $\xi_i = \frac{n_{3,i}}{\sqrt{\Delta s}}$ where $n_{3,i+1}$ is the standard i.i.d. normal random variable. The Ornstein–Uhlenbeck process is simulated by the scheme proposed in [49],

$$\xi_{i+1} = \xi_i e^{-\gamma\Delta s} + \sigma\sqrt{\frac{(1-e^{-2\gamma\Delta s})}{2\gamma}}n_{3,i+1}, \tag{32}$$

where γ, σ are the damping parameter and the dispersion parameter of the OU process, respectively. For each realization of $\xi(s)$, we use 10^6 independent SDE solutions $(X_t(s), Y_t(s))$ to compute the path integral representation of $T(x, y, t)$. For the cases presented in Fig. 4, we need 300 time steps for reaching the long time asymptotic state. The simulations are performed on UNC's Longleaf computing cluster with 400 parallel computing jobs, and each job takes approximately 3 days on the cluster.

A.2. Lists of abbreviations

See Table 1.

References

[1] R.M. McLaughlin, A.J. Majda, An explicit example with non-Gaussian probability distribution for nontrivial scalar mean and fluctuation, Phys. Fluids 8 (1996) 536–547.
[2] E. Balkovsky, G. Falkovich, Two complementary descriptions of intermittency, Phys. Rev. E 57 (1998) R1231.
[3] M. Chertkov, G. Falkovich, I. Kolokolov, Intermittent dissipation of a passive scalar in turbulence, Phys. Rev. Lett. 80 (1998) 2121.
[4] Y.G. Sinai, V. Yakhot, Limiting probability distributions of a passive scalar in a random velocity field, Phys. Rev. Lett. 63 (1989) 1962.
[5] P.W. Anderson, Absence of diffusion in certain random lattices, Phys. Rev. 109 (1958) 1492.
[6] J.C. Bronski, D.W. McLaughlin, M.J. Shelley, On the stability of time-harmonic localized states in a disordered nonlinear medium, J. Stat. Phys. 88 (1997) 1077–1115.
[7] M.J. Stephen, Temporal fluctuations in wave propagation in random media, Phys. Rev. B 37 (1988) 1.
[8] C.T. Bolles, K. Speer, M. Moore, Anomalous wave statistics induced by abrupt depth change, Phys. Rev. Fluids 4 (2019) 011801.
[9] A.J. Majda, M. Moore, D. Qi, Statistical dynamical model to predict extreme events and anomalous features in shallow water waves with abrupt depth change, Proc. Natl. Acad. Sci. 116 (2019) 3982–3987.
[10] B. Castaing, G. Gunaratne, F. Heslot, L. Kadanoff, A. Libchaber, S. Thomae, X.Z. Wu, S. Zaleski, G. Zanetti, Scaling of hard thermal turbulence in Rayleigh–Bénard convection, J. Fluid Mech. 204 (1989) 1–30.
[11] V. Yakhot, S.A. Orszag, S. Balachandar, E. Jackson, Z.S. She, L. Sirovich, Phenomenological theory of probability distributions in turbulence, J. Sci. Comput. 5 (1990) 199–221.
[12] A. Pumir, B.I. Shraiman, E.D. Siggia, Exponential tails and random advection, Phys. Rev. Lett. 66 (1991) 2984.
[13] A.R. Kerstein, Linear-eddy modelling of turbulent transport. Part 6. Microstructure of diffusive scalar mixing fields, J. Fluid Mech. 231 (1991) 361–394.
[14] Y. Kimura, R.H. Kraichnan, Statistics of an advected passive scalar, Phys. Fluids A 5 (1993) 2264–2277.
[15] E.S. Ching, Y. Tu, Passive scalar fluctuations with and without a mean gradient: A numerical study, Phys. Rev. E 49 (1994) 1278.
[16] A.J. Majda, The random uniform shear layer: an explicit example of turbulent diffusion with broad tail probability distributions, Phys. Fluids A 5 (1993) 1963–1970.
[17] A.J. Majda, Explicit inertial range renormalization theory in a model for turbulent diffusion, J. Stat. Phys. 73 (1993) 515–542.
[18] J. Bronski, R. McLaughlin, Passive scalar intermittency and the ground state of Schrödinger operators, Phys. Fluids 9 (1997) 181–190.
[19] J.C. Bronski, R.M. McLaughlin, Rigorous estimates of the tails of the probability distribution function for the random linear shear model, J. Stat. Phys. 98 (2000) 897–915.
[20] R.H. Kraichnan, Small-scale structure of a scalar field convected by turbulence, Phys. Fluids 11 (1968) 945–953.
[21] J.C. Bronski, R.M. McLaughlin, The problem of moments and the Majda model for scalar intermittency, Phys. Lett. A 265 (2000) 257–263.
[22] S.G. Resnick, Dynamical Problems in Non-Linear Advective Partial Differential Equations (Ph.D. thesis), The University of Chicago, 1996.
[23] E. Vanden Eijnden, Non-Gaussian invariant measures for the Majda model of decaying turbulent transport, Comm. Pure Appl. Math. 54 (2001) 1146–1167.
[24] R. Antonia, K. Sreenivasan, Log-normality of temperature dissipation in a turbulent boundary layer, Phys. Fluids 20 (1977) 1800–1804.
[25] L. Sparling, J. Bacmeister, Scale dependence of tracer microstructure: PDFs, intermittency and the dissipation scale, Geophys. Res. Lett. 28 (2001) 2823–2826.
[26] R. Camassa, Z. Lin, R.M. McLaughlin, Evolution of the probability measure for the Majda model: New invariant measures and breathing PDFs, J. Stat. Phys. 130 (2008) 343–371.
[27] J.C. Bronski, R. Camassa, Z. Lin, R.M. McLaughlin, A. Scotti, An explicit family of probability measures for passive scalar diffusion in a random flow, J. Stat. Phys. 128 (2007) 927–968.
[28] R. Camassa, Z. Kilic, R.M. McLaughlin, On the symmetry properties of a random passive scalar with and without boundaries, and their connection between hot and cold states, Physica D 400 (2019) 132124.
[29] G.I. Taylor, Dispersion of soluble matter in solvent flowing slowly through a tube, Proc. R. Soc. A 219 (1953) 186–203.
[30] R. Aris, On the dispersion of a solute in a fluid flowing through a tube, Proc. R. Soc. A 235 (1956) 67–77.
[31] L. Ding, R. Hunt, H. Woodie, R.M. McLaughlin, Enhanced diffusivity and skewness of a diffusing tracer in the presence of an oscillating wall, Res. Math. Sci. 8 (3) (2021) 34.
[32] I. Karatzas, S. Shreve, Brownian Motion and Stochastic Calculus, Vol. 113, Springer, 2014.

[33] T. Inglot, P. Majerski, Simple upper and lower bounds for the multivariate Laplace approximation, J. Approx. Theory 186 (2014) 1–11.
[34] W.A. Strauss, Partial Differential Equations: An Introduction, John Wiley & Sons, 2007.
[35] J. Sherman, W.J. Morrison, Adjustment of an inverse matrix corresponding to a change in one element of a given matrix, Ann. Math. Stat. 21 (1950) 124–127.
[36] G. Mercer, A. Roberts, A centre manifold description of contaminant dispersion in channels with varying flow properties, SIAM J. Appl. Math. 50 (1990) 1547–1565.
[37] J. Bedrossian, M.C. Zelati, Enhanced dissipation, hypoellipticity, and anomalous small noise inviscid limits in shear flows, Arch. Ration. Mech. Anal. 224 (3) (2017) 1161–1204.
[38] M. Beck, O. Chaudhary, C.E. Wayne, Analysis of enhanced diffusion in Taylor dispersion via a model problem, in: Hamiltonian Partial Differential Equations and Applications, 2015, pp. 31–71.
[39] M. Beck, O. Chaudhary, C.E. Wayne, Rigorous justification of Taylor dispersion via center manifolds and hypocoercivity, Arch. Ration. Mech. Anal. 235 (2020) 1105–1149.
[40] Z. Kilic, Random Transport of Passive Scalars (Ph.D. thesis), Applied Mathematics Program, UNC at Chapel Hill, 2018.
[41] J. Bedrossian, A. Blumenthal, S. Punshon-Smith, The batchelor spectrum of passive scalar turbulence in stochastic fluid mechanics, 2019, arXiv preprint arXiv:1911.11014.
[42] Z. Lin, K. Boďová, C.R. Doering, Models & measures of mixing & effective diffusion, Discrete Contin. Dyn. Syst. A 28 (1) (2010) 259.
[43] A. Bourlioux, A. Majda, Elementary models with probability distribution function intermittency for passive scalars with a mean gradient, Phys. Fluids 14 (2) (2002) 881–897.
[44] M. Avellaneda, A.J. Majda, Renormalization theory for eddy diffusivity in turbulent transport, Phys. Rev. Lett. 68 (20) (1992) 3028.
[45] M. Avellaneda, A.J. Majda, Mathematical models with exact renormalization for turbulent transport, Comm. Math. Phys. 131 (2) (1990) 381–429.
[46] R. Camassa, R.M. McLaughlin, C. Viotti, Analysis of passive scalar advection in parallel shear flows: sorting of modes at intermediate time scales, Phys. Fluids 22 (11) (2010) 117103.
[47] S. Rosencrans, Taylor dispersion in curved channels, SIAM J. Appl. Math. 57 (5) (1997) 1216–1241.
[48] G. Marsaglia, T.A. Bray, A convenient method for generating normal variables, SIAM Rev. 6 (1964) 260–264.
[49] D.T. Gillespie, Exact numerical simulation of the Ornstein–Uhlenbeck process and its integral, Phys. Rev. E 54 (1996) 2084.